

# Revealing Modular Architecture of Human Brain Structural Networks by Using Cortical Thickness from MRI

Zhang J. Chen, Yong He, Pedro Rosa-Neto, Jurgen Germann and Alan C. Evans

McConnell Brain Imaging Centre, Montreal Neurological Institute, McGill University, Montreal, QC, Canada H3A 2B4

**Modularity, presumably shaped by evolutionary constraints, underlies the functionality of most complex networks ranged from social to biological networks. However, it remains largely unknown in human cortical networks. In a previous study, we demonstrated a network of correlations of cortical thickness among specific cortical areas and speculated that these correlations reflected an underlying structural connectivity among those brain regions. Here, we further investigated the intrinsic modular architecture of the human brain network derived from cortical thickness measurement. Modules were defined as groups of cortical regions that are connected morphologically to achieve the maximum network modularity. We show that the human cortical network is organized into 6 topological modules that closely overlap known functional domains such as auditory/language, strategic/executive, sensorimotor, visual, and mnemonic processing. The identified structure-based modular architecture may provide new insights into the functionality of cortical regions and connections between structural brain modules. This study provides the first report of modular architecture of the structural network in the human brain using cortical thickness measurements.**

**Keywords:** betweenness centrality, cortical thickness, modularity, morphometry, MRI, network, small world

## Introduction

Modularity is one of the most important features of most complex systems in nature, ranging from social to biological networks (Hartwell et al. 1999; Newman 2006). Detecting modules in a network may help us to identify relevant substructures that correspond to important functions providing a link between structure and function in complex networks (Fortunato and Barthelemy 2007). In neuroscience, network analysis has provided rich quantitative insights into the organization, development, and function of complex brain networks (Sporns et al. 2004). Evidence from mammalian brain network studies (Hilgetag et al. 2000; Zhou et al. 2006) has presupposed potential modularity in the topology of the human cortical network. However, defining and identifying structure-based functional modules in the human cortical network has proved to be challenging because of an incomplete understanding of the structural-functional mapping and network of anatomical connections linking the neuronal elements of the human brain known as the human “connectome” (Sporns et al. 2005).

Currently, human cortical network research has been mainly focused on functional connectivity patterns analysis using neurophysiological data collected from functional magnetic resonance imaging (fMRI) (Salvador et al. 2005; Achard et al. 2006; Achard and Bullmore 2007), electroencephalogram

(Micheloyannis et al. 2006; Stam et al. 2007), magnetoencephalogram (Stam 2004; Bassett et al. 2006). Accessible and ubiquitous cortical morphometric data have been generally overlooked and seldom studied in brain network analysis to date. Recent studies have suggested that, at macroscale, interregional statistical associations in cortical thickness (a composite measurement of size, density, and arrangement of cortical neurons, neuroglia, and nerve fibers) (Parent and Carpenter 1995) reveal important structural connectivity information in the human brain (Lerch et al. 2006; He, Chen, et al. 2007). We have demonstrated, using a graph theoretical network analysis (GRETNA) algorithm, that coordinated variations in cortical thickness exhibit small-world attributes characterized by cohesive neighborhoods with high clustering and short mean distance between regions that reflect a near-optimal organizational pattern of anatomical network in the human brain. Such interregional correlations in cortical thickness might arise from the interaction between underlying neuronal substrates through their anatomical connections.

In the present study, we investigated the modularity of a cortical network consisting of 45 regions and 102 significant connections that was constructed in our previous study using MRI data from 124 normal adults (He, Chen, et al. 2007). We hypothesize that the connectivity pattern of morphological variations in the thickness of cerebral cortex reveals an intrinsic modularity wherein tight coupling within subgroups of cortical regions (modules) within the overall network reflects the functional organization of the brain. Finally, the topological importance of specific cortical regions and paths are also evaluated in terms of their contribution to network properties.

## Materials and Methods

### Subjects and MRI Acquisition

One hundred and twenty-four right-handed subjects (male/female = 71/53,  $24.38 \pm 4.25$  y) were drawn from the International Consortium for Brain Mapping database (Mazziotta et al. 2001). Each subject provided written consent, and the study was approved by the Research Ethics Committee of the Montreal Neurological Institute and Hospital. The MRI scans were performed on a Philips Gyroscan 1.5T superconducting magnet system. T1, T2, and proton density images were collected though only T1 images (1 mm isotropic, time repetition = 18 ms, time echo = 10 ms, flip angle =  $30^\circ$ ) were analyzed in this study. The detailed characteristics of the subjects and description of the scanning sequences can be found in Watkins et al. 2001 and He, Chen, et al. 2007.

### Human Brain Structural Network Construction Using Cortical Thickness

Images preprocessing procedures, cortical thickness measurements, and cortical thickness network construction have been previously

described (He, Chen, et al. 2007). In brief, to obtain the binarized and undirected cortical thickness connectivity matrix as shown in Figure 1a, we computed the Pearson correlation coefficients ( $R$ ) between regional thicknesses across subjects and thresholded interregional thickness matrix using a false discovery rate procedure (Genovese et al. 2002). The final human brain structural network derived from cortical thickness measurements contains 45 connected cortical regions and 102 connections (Fig. 1a).

### Network Modularity ( $Q$ )

The modularity measure  $Q(p)$  for a given partition  $p$  of the human brain structural brain network is defined (Guimera and Sales-Pardo 2006; Newman 2006) as

$$Q(p) = \sum_{s=1}^N \left[ \frac{l_s}{L} - \left( \frac{d_s}{2L} \right)^2 \right], \quad (1)$$

where  $N$  is the number of modules,  $L$  is the number of connections in the network,  $l_s$  is the number of connections between nodes in module  $s$ , and  $d_s$  is the sum of the degrees of the nodes in module  $s$ . The modularity,  $Q$ , quantifies the difference between the actual number of intramodule links and the expected number for the same modules in a randomized network (Danon et al. 2006). The objective of a modular detection algorithm is to find the partition  $p$  that maximizes this network modularity  $Q$  as higher  $Q$  indicates a strong partition of the network (Guimera and Sales-Pardo 2006). In practice, a  $Q$  value above 0.3 is a good indicator of significant modules in a network (Clauset et al. 2004).

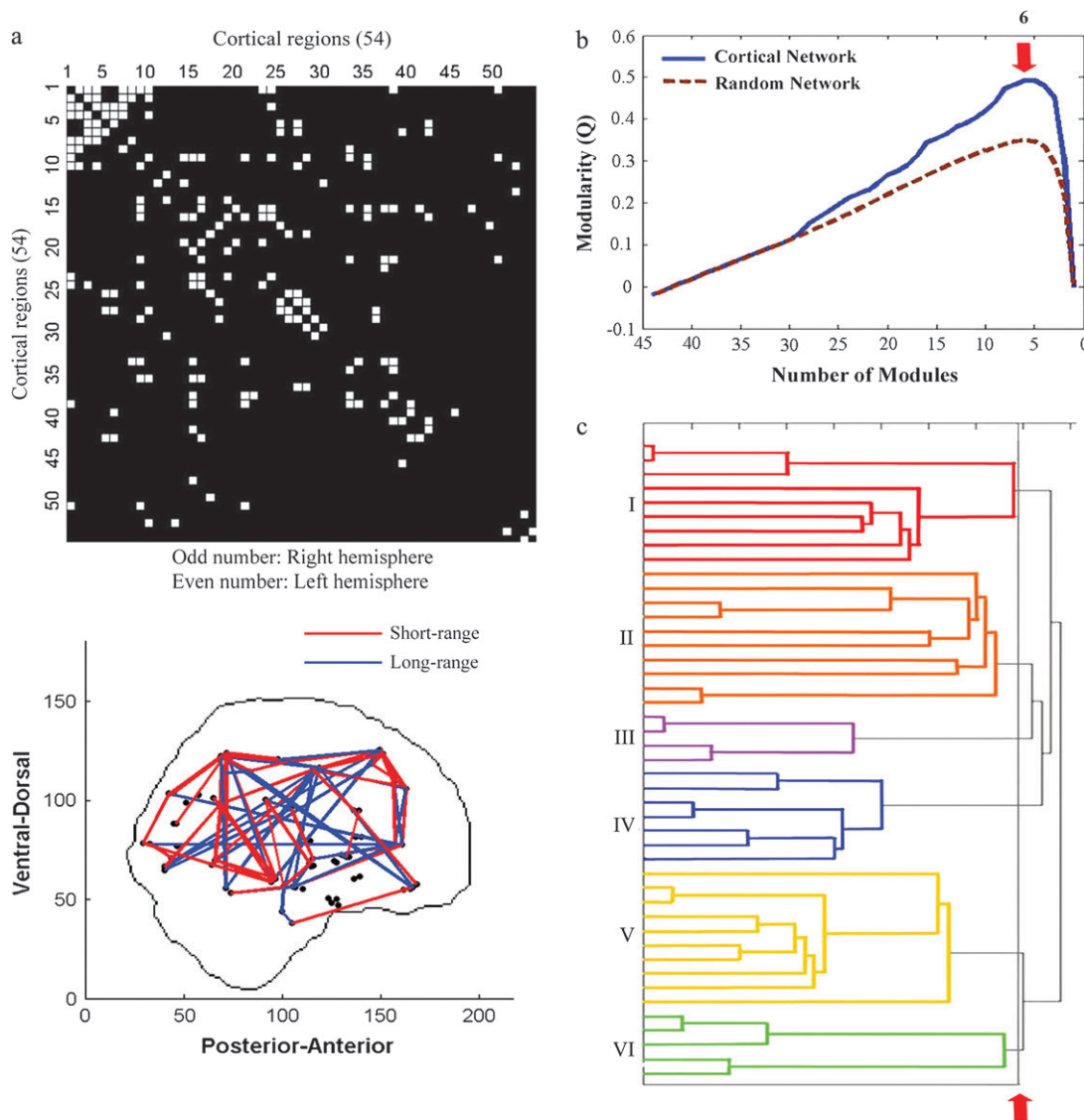


**Figure 1.** Identification of the functional modules in the human brain structural network. (a) (Top panel) The binarized matrix represents the human brain structural network constructed using cortical thickness from MRI (He, Chen, et al. 2007). (Bottom panel) Each suprathreshold cell in the top panel represents 1 “link” in the brain network. (1,2) SFG, (3,4) MFG, (5,6) IFG, (7,8) MdFG, (9,10) PrCG, (11,12) LOFG: lateral fronto-orbital gyrus, (13,14) MOFG, (15,16) SPL, (17,18) SMG, (19,20) ANG: angular gyrus, (21,22) PCU: precuneus gyrus, (23,24) PoCG, (25,26) STG, (27,28) MTG, (29,30) ITG: inferior temporal gyrus, (31,32) UNC: uncus, (33,34) MOTG: medial occipitotemporal gyrus, (35,36) LOTG, (37,38) PHG: parahippocampal gyrus, (39,40) OP: occipital pole, (41,42) SOG: superior occipital gyrus, (43,44) MOG: middle occipital gyrus, (45,46) IOG: inferior occipital gyrus, (47,48) CUN: cuneus, (49,50) LING, (51,52) CING: cingulate region, (53,54) INS: insula. (b) Progress of the network modularity,  $Q$ , as regions are merged into modules for the human cortical network (blue) and 1000 random networks (dotted). Red down arrow indicates the cortical network modularity reaches maximum when the network is segmented into 6 modules ( $Z$  score = 7.9). The network modularity decreases as the merge continues indicating a less optimized network modular organization. (c) Dendrogram representation of the modules identification progress determined by modularity ( $Q$ ). The maximum  $Q$  is reached when the network is separated into 6 modules indicated by the red up arrow.

### Network Modularity ( $Q$ ) Optimization

To identify modules of the brain structural network (Fig. 1*a*) that optimize the network modularity defined in equation (1), we implement a greedy optimization algorithm (Danon et al. 2006). The algorithm is based on Newman's fast algorithm (Clauset et al. 2004; Newman 2004) that is similar to the standard agglomerative hierarchical clustering technique.

We first start with a state in which each cortical region (node) in the human brain structural network (Fig. 1*a*) is the sole member of a module  $i$ . Hence, the initial network modularity  $Q$  can be computed as

$$Q = \sum_i (e_{ii} - a_i^2), \quad (2)$$

where:  $e_{ii}$  (0 initially) is the fraction of all edges that connect vertices within module  $i$ ,  $a_i$  is the proportion of links belonging to module  $i$  (degree of module  $i$ ) over total number of network links.

An initial modularity matrix is then constructed from equation (2) as

$$\Delta Q_{ij} = \begin{cases} 2(e_{ij} - a_i a_j), & \text{if } i, j \text{ are connected,} \\ 0, & \text{otherwise,} \end{cases} \quad (3)$$

where  $e_{ij}$  is the fraction of edges in the network that connect vertices in module  $i$  to those in module  $j$  which is 1 over the total number of network links if  $i$  and  $j$  are connected initially.  $a_i$  and  $a_j$  are denoted as the proportion of links belonging to the module  $i$  and  $j$  which is the degree of modules (nodes)  $i$  and  $j$  over total number of network links, respectively. This is a measurement of affinity between modules  $i$  and  $j$  as the higher  $\Delta Q_{ij}$  becomes, the more likely modules  $i$  and  $j$  belong to the same module.

The algorithm joins modules together in pairs choosing at each step the pairing that results in the greatest increase in  $Q$  determined by a normalized  $\Delta Q_{ij}$ , (Danon et al. 2006):

$$\Delta Q_{ij} = \frac{2}{a_i} (e_{ij} - a_i a_j). \quad (4)$$

This normalization insures that clusters with fewer links have largest values of  $\Delta Q_{ij}$ , and therefore are joined earlier (Danon et al. 2006). The advantage of this optimization approach is that it takes into account of the heterogeneity of module size observed in real networks (Danon et al. 2006). The algorithm stops the modules joining process when  $\Delta Q_{ij}$  become negative because the agglomeration is no longer contributing to the optimization of the network modularity.

### Statistical Significance

The nontrivial distributions of the cortical network also raise the question as to whether the observed maximum network modularity is statistically significant compared with that of comparable random graphs. In other words, what happens with the modularity of the cortical network if the links of the network are randomly reorganized?

To address this issue, random graphs were generated that preserved the degree distribution of the real network (Maslov and Sneppen 2002). We defined  $Z$  score as  $(Q_{\text{real}} - Q_{\text{rand}})/Q_{\text{std}}$ , where  $Q_{\text{real}}$  is the maximum modularity of the cortical network and  $Q_{\text{rand}}$  and  $Q_{\text{std}}$  are the average maximum modularity and standard deviations of the maximum modularity over 1000 randomized networks, respectively.

### Node and Edge Betweenness Centrality

The concept of betweenness centrality is a powerful tool in identifying pivotal nodes and edges, with respect to information flow, within a network (Freeman 1977; Girvan and Newman 2002). The betweenness of a node  $N_{bc}(v)$  is defined as the number of shortest paths between pairs of other nodes that pass through the node.

$$N_{bc}(v) = \sum_{s \neq v \neq t \in V} \frac{\sigma_{st}(v)}{\sigma_{st}}, \quad (5)$$

where  $V$  is the set of nodes in the network,  $\sigma_{st}$  is the number of shortest geodesic paths from  $s$  to  $t$ , and  $\sigma_{st}(v)$  is the number of shortest geodesic paths from vertex  $s$  to vertex  $t$  that pass through the vertex  $v$ . The *relative* betweenness centrality of a node is its centrality divided by the maximum node centrality of the network.

In an analogous manner, the betweenness of an edge  $E_{bc}(\{k, k'\})$  is defined as the number of shortest paths between pairs of other nodes that pass through the edge.

$$E_{bc}(\{k, k'\}) = \sum_{\substack{s \neq t \in V, \\ \{s, t\} \neq \{k, k'\}}} \frac{\sigma_{st}(\{k, k'\})}{\sigma_{st}}, \quad (6)$$

where  $V$  is the group of vertices in the network,  $\sigma_{st}$  is the number of shortest geodesic paths from  $s$  to  $t$ , and  $\sigma_{st}(\{k, k'\})$  is the number of shortest geodesic paths from vertex  $s$  to vertex  $t$  that pass through the edge  $\{k, k'\}$ . The relative betweenness centrality of an edge is its centrality divided by the maximum edge centrality of the network.

The relative betweenness centrality of nodes and edges in this study are measured using MatlabBGL v2.1 ([http://www.stanford.edu/~dgleich/programs/matlab\\_bgl/](http://www.stanford.edu/~dgleich/programs/matlab_bgl/)).

## Results

### Cortical Network Modularity

Based on our previous study in the small-world attributes (high clustering coefficient and short mean path lengths) of the structural brain network (He, Chen, et al. 2007), we hypothesized that the high clustering is also an indication of a potential high modularity ( $Q$ ) (Newman 2006). The objective of module detection is to find the partitions that maximize the brain network modularity  $Q$  (see Materials and Methods). The module detection algorithm was applied directly on the binarized structural brain network constructed from cortical thickness measurements (He, Chen, et al. 2007) as shown in Figure 1*a*. Figure 1*b* demonstrated the progress of  $Q$  as regions are merged into modules for the human cortical network (blue line) and 1000 matched random networks (dotted line). Figure 1*c* is the dendrogram representation of the modules identification progress along with the modularity ( $Q$ ) measurements. The maximum modularity ( $Q = 0.5$ ,  $Z$ score = 7.9) was reached when the cortical network was separated into 6 modules indicated by the red arrows (Fig. 1*b,c*). The statistically significant modularity of the cortical network implies that the underlying modular architecture arises from specific interactions among cortical regions.

### Functional Significance of Network Modules

We referred to cortical network modules as groups of cortical regions that are both connected morphologically and subserving distinct brain functions such as language, motor, and visual functions. Each module in a network should have denser intramodule connections than its intermodule connections. The identification of modules of connected regions (based entirely upon correlations of regional cortical thickness) was quantified by modularity (Newman 2006) and obtained without any prior knowledge of regional functions. Six structure-based modules, consisted of 4–10 cortical regions, were identified at the maximum network modularity (Danon et al. 2006) (Fig. 2).

Modules were labeled from I to VI as shown in Figure 1 and Figure 2. Module I (red) consists of 9 regions mostly from prefrontal areas such as bilateral superior frontal gyrus (SFG), middle frontal gyrus (MFG), and medial frontal gyrus (MdFG) that are known to be primarily involved in strategic/executive functions (Duncan and Owen 2000). The 10-region module II (orange) found in the network includes regions mostly from (pre)motor and parietal cortices such as left precentral gyrus (PrCG), bilateral superior parietal lobule (SPL), angular gyrus, and postcentral gyrus (PoCG) that are mainly associated with sensorimotor/spatial functions (Mesulam 2000). The other 10-region module V (yellow) includes bilateral supramarginal

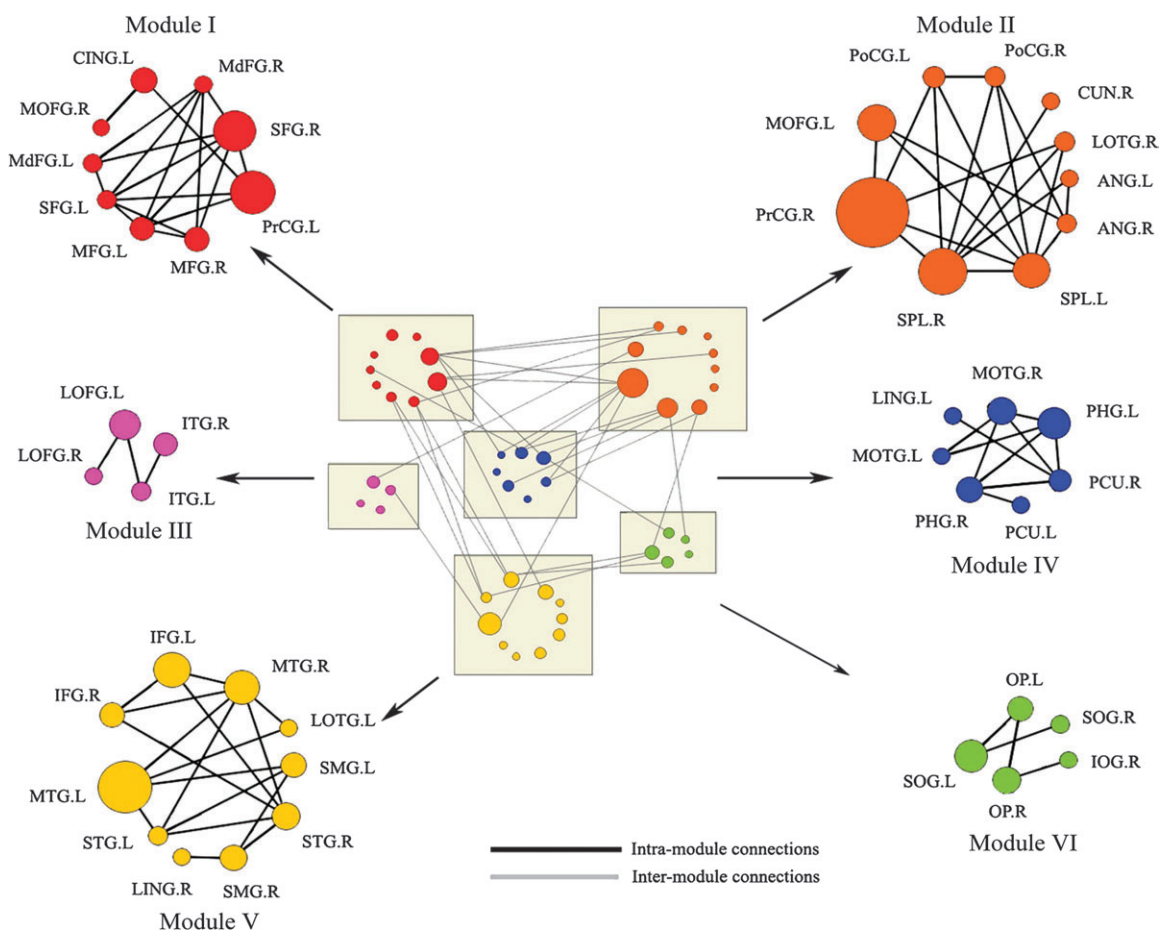


**Figure 2.** Modular architecture of the human cortical network. Six modules of human cortical network displayed in groups. Red: module I, orange: module II, pink: module III, blue: module IV, yellow: module V, green: module VI. The intermodule connections and intramodular connections of the network are shown in dark and gray lines, respectively. The size of each node denotes the relative betweenness centrality ( $N_{bc}$ ) of the cortical region in the brain network (for details, see Table 1).

gyrus (SMG), middle temporal gyrus (MTG), superior temporal gyrus (STG), and inferior frontal gyrus (IFG), all of which can be associated with auditory/language functions (Mesulam 1990). Module VI (green) is composed of 5 regions from the occipital lobe that are specialized for visual processing. The 4-member module III (pink) includes bilateral lateral frontoorbital gyrus and inferior temporal gyrus that are connected through the uncinate fasciculus (Kier et al. 2004) and could also be part of olfactocentric system (Mesulam 1985). Module IV (blue) includes regions such as bilateral parahippocampal gyrus, pre-cuneus, and medial occipitotemporal gyrus that are associated with mnemonic and emotion processing (Mesulam 1990; Cavanna and Trimble 2006).

There were also some functionally less studied cortical regions within each module. For example, both left lateral occipitotemporal gyrus (LOTG) and right lingual gyrus (LING) are found in the auditory/language module V as both regions are linked to the phonological analysis of speech, an essential component of language processing for mapping sound information onto higher levels of language process (Burton et al. 2005). On the other hand, a recent fMRI study has revealed significant activation in the right LOTG (module II) in detecting motion, object form, and human body form (Downing et al. 2007). Isenberg et al. (1999) proposed that left LING (module IV) is modulated by the amygdala along with parahippocampal region

to subserve enhanced semantic encoding. Although a unique functionality for each cortical region is difficult to define and can be ambiguous at times, the results nevertheless demonstrate strong connections among cortical regions within each module of the human brain structural network.

#### Nodes Betweenness Centrality

We calculated the relative nodal betweenness centrality ( $N_{bc}$ ) of each region in the cortical network (mean = 0.173). Cortical regions with high  $N_{bc}$  are important in managing the flow of information across the network because they are more likely to reside on the shortest path between other regions. The relative  $N_{bc}$  of each region is represented by the size of each circle in Figure 2, and the associations between  $N_{bc}$  of each cortical region and its intermodular connections are shown in Table 1. We found that regions with high  $N_{bc}$  ( $>0.173$ ) are predominately intermodular connectors located in the regions of the parietal, temporal, and frontal heteromodal association cortex (SPL, SMG, MTG, STG, IFG, and SFG) (Mesulam 2000) and highly connected primary motor cortex (PrCG) (Luppino and Rizzolatti 2000).

#### Edges Betweenness Centrality

Similar to the  $N_{bc}$ , edge betweenness centrality ( $E_{bc}$ ) identifies critical paths in the brain structural network.

**Table 1**

Regions of human brain cortical network and their associated modules sorted in the order of decreasing betweenness centrality

Abbreviation	Class	$N_{bc}(V)$	Module	Module No. (regions)
<b>PrCG.R</b>	Primary	1.000	II	I(1,10), IV(21,33,50), V(28)
<b>MTG.L</b>	Association	0.667	V	II(9), III(29)
<b>SPL.R</b>	Association	0.555	II	IV(33,37,38), VI(41)
<b>PrCG.L</b>	Primary	0.504	I	II(9,35), V(27)
<b>SFG.R</b>	Association	0.455	I	II(9,23,24), IV(38,50)
<b>MOFG.L</b>	Paralimbic	0.366	II	III(12)
<b>IFG.L</b>	Association	0.354	V	I(3,4), VI(39,42)
<b>SPL.L</b>	Association	0.346	II	IV(21), VI(42)
<b>MTG.R</b>	Association	0.329	V	I(10)
<b>PHG.L</b>	Paralimbic	0.281	IV	I(1), II(15), VI(40)
<b>SOG.L</b>	Association	0.280	VI	II(16), V(5,6)
<b>LOFG.L</b>	Paralimbic	0.239	III	II(14)
<b>MOTG.R</b>	Association	0.204	IV	I(8), II(9,15)
<b>STG.R</b>	Association	0.196	V	N/A
<b>OP.R</b>	Primary	0.183	VI	V(6)
<b>SMG.R</b>	Association	0.174	V	N/A
PHG.R	Paralimbic	0.168	IV	II(15)
CING.L	Association	0.165	I	N/A
SMG.L	Association	0.150	V	N/A
MFG.R	Association	0.142	I	II(24), V(5,6)
IFG.R	Association	0.140	V	I(3,4), VI(42)
OP.L	Primary	0.140	VI	IV(38)
MFG.L	Association	0.127	I	V(5,6)
ITG.R	Association	0.114	III	V(28)
PCU.R	Paralimbic	0.095	IV	II(9,16)
PoCG.L	Primary	0.089	II	I(1,3)
PoCG.R	Primary	0.053	II	I(1)
LOTG.R	Association	0.050	II	I(10)
ITG.L	Association	0.039	III	N/A
STG.L	Association	0.037	V	N/A
SFG.L	Association	0.034	I	N/A
ANG.R	Association	0.034	II	N/A
MdFG.L	Association	0.032	I	IV(33)
SOG.R	Association	0.020	VI	II(15)
MdFG.R	Association	0.013	I	N/A
ANG.L	Association	0.008	II	N/A
LING.L	Association	0.005	IV	I(1), II(9)
LOFG.R	Paralimbic	0.000	III	N/A
MOFG.R	Paralimbic	0.000	I	N/A
PCU.L	Paralimbic	0.000	IV	N/A
MOTG.L	Association	0.000	IV	N/A
LOTG.L	Association	0.000	V	N/A
IOG.R	Association	0.000	VI	N/A
CUN.R	Association	0.000	II	N/A
LING.R	Association	0.000	V	N/A

Cortical regions with intermodular connections (shaded) in the human brain structural network were identified from their modular organization and sorted in order of decreasing relative node betweenness  $N_{bc}$  (see Fig. 1 for the abbreviations). Regions with higher than mean network betweenness centrality (0.173) are also identified (in bold). All regions were classified as primary, associations, and paralimbic as described in He, Chen, et al., 2007. The module classification of each region (I–VI) is according to Figure 2. The intermodular connections associated with each cortical region are listed in the last column as module no. where numbers in brackets represent the other cortical regions that connect to that region (see Fig. 1 for the region names). R, right; L, left; PHG, parahippocampal gyrus; SOG, superior occipital gyrus; LOFG, lateral fronto-orbital gyrus; MOTG, medial occipitotemporal gyrus; OP, occipital pole; CING, cingulate region; ITG, inferior temporal gyrus; ANG, angular gyrus; IOG, inferior occipital gyrus; CUN, cuneus.

Network paths with high  $E_{bc}$  are more likely to reside on the shortest path between any 2 regions. Table 2 demonstrated the top 15 ranked connections (see Supplementary Table for a full list of the paths). We found that paths with high  $E_{bc}$  are more likely to be intermodular connections (10/15; 67%) that connect regions with high  $N_{bc}$  indicated in previous section (e.g., PrCG, MTG, SPL, and SFG) despite majority of paths (72/102; 71%) are intramodular connections. In addition, we also observed some intramodular paths with high  $E_{bc}$  actually connect high  $N_{bc}$  regions with low  $N_{bc}$  (<0.173) regions such as the MTG.L–SMG.L and PrCG.L–cingulate region (CING.L) links (Table 2).

**Table 2**

The top 15 ranked cortical network paths in betweenness centrality and their connected modules

Region A	Region B	$E_{bc}(\{k,k'\})$	Modules
PrCG.R	MTG.L	1.000	II–V
LOFG.L	MOFG.L	0.590	II–III
PrCG.L	CING.L	0.539	I
PrCG.R	MOFG.L	0.512	II
SMG.L	MTG.L	0.445	V
MTG.L	ITG.R	0.438	V–III
PrCG.R	SPL.R	0.405	II
SPL.L	SOG.L	0.405	II–VI
PrCG.L	MTG.R	0.400	I–V
IFG.L	OP.R	0.370	V–VI
PrCG.R	PrCG.L	0.366	II–I
PrCG.R	MOTG.R	0.336	II–IV
PHG.L	OP.L	0.314	IV–VI
SFG.R	PHG.L	0.313	I–IV
SMG.R	STG.R	0.295	V

List of the top 15 ranked paths with a network edge betweenness centrality greater than the mean (0.186) are identified and listed in order of decreasing relative edge betweenness  $E_{bc}$  (see Fig. 1 for the abbreviations and Supplementary Table for the full list) in the human brain structural network. Modules column shows the 2 cortical network modules that each path (intermodular connection) is connected to or the module that each path (intramodular connection) belongs to. R, right; L, left; LOFG, lateral fronto-orbital gyrus; CING, cingulate region; ITG, inferior temporal gyrus; SOG, superior occipital gyrus; OP, occipital pole; MOTG, medial occipitotemporal gyrus; PHG, parahippocampal gyrus.

## Discussion

This is the first study to demonstrate the modular architecture of the large-scale structural connectivity patterns in the entire human cerebral cortex using cortical thickness measurements. The segregation of brain regions into 6 modules with functional significance suggests that functional organization of human brain networks has a modularized anatomical consequence. In addition, we also showed that cortical regions and paths with high betweenness centrality are most likely to be the intermodular connectors and connections, respectively. Taken together, our results provide a detailed view of modular organization of the human brain structural network.

### Modular Architecture of the Human Brain Structural Network

We have proposed a modular architecture for the human brain structural network that is composed of groups of tightly connected cortical regions. This analysis is based on our previous findings of small-world network properties (high clustering and short mean paths length between nodes) in the human brain structural network using cortical thickness (He, Chen, et al. 2007). High clustering represents a general organizational principle throughout many large-scale brain networks (Sporns et al. 2004) and may contribute to the balance between brain functional segregation and integration while conserving connections length (Sporns et al. 2000), efficient recurrent processing within modules (Sporns et al. 2000; Kotter and Stephan 2003), and efficient information exchange between modules (Latora and Marchiori 2001). Prior studies in the mammalian and human brain networks have revealed clusters that closely overlap with known brain functions (Hilgetag et al. 2000; Salvador et al. 2005; Zhou et al. 2006). Consistent with these principles, the organization of the human structural brain network shown here reflects an intrinsic modularity of the functional organization of the brain.

We identified 6 modules in the human brain structural network corresponding to 6 general brain functional domains (see Results). Those results are compatible with functional

modules detected in the mammalian anatomical network (visual, auditory, somatosensory/motor, frontal/limbic) (Scannell et al. 1995; Scannell et al. 1999; Hilgetag et al. 2000). However, one distinctive difference between the human and mammalian cortical structural networks is the appearance of strong language module (V) in the human cortical network, which supports the notion that language ability is what sets us apart from other animals (Lieberman 1998). Our findings might provide a structural basis for the differences in the functional organization of the human and mammalian brain networks.

The modular architecture of human brain structural network is also consistent with the functional network of human brain. A recent fMRI study has suggested that, in the resting state, the functional architecture of the normal human brain displays a similar modular pattern (spatial/motor, executive, visual, auditory-verbal, paralimbic) (Salvador et al. 2005). However, our study provides the first evidence of a modularized structural organization underlying the functional connectivity pattern of the human brain network.

The GRETNA above also demonstrated that the modular architecture of the human structural network is comparable to functional correlations between most bilaterally homologous regions (e.g., SFG, STG, SMG, PoCG, etc.) as they are consistently grouped together in the same module (Fig. 2 and Table 1). Previous human brain functional studies have demonstrated strong functional correlations between bilaterally homologous regions (Lowe et al. 1998; Hampson et al. 2002; Wang et al. 2006) and a similar symmetric clustering connectivity pattern (Salvador et al. 2005), presumably resulted from the interhemispheric callosal connections. A recent study showed significant correlations between bilateral regional gray matter density (Mechelli et al. 2005). One exceptional observation concerns the PrCG regions that are found in different modules (left: I; right: II). However, the functional and structural asymmetries of the primary motor cortex was well documented (Amunts et al. 1996) and found to be related to a hemispheric asymmetry in motor control (left: regulation of motor behavior; right: spatial functions) (Serrien et al. 2006).

The assignment of functionally annotated cortical regions to their corresponding modules in our results is consistent with well-known brain functional systems. Thus, the network modules identified provide a functional anatomy for different cortical regions including areas with less defined functions and asymmetrically categorized. The structural description of the cortical network elements might provide new insights into the understanding of how brain functions emerge from their underlying structural substrates (Sporns et al. 2005). Though, further experimental and analyses are needed to understand the role of each cortical region within its module.

We also examined the topological importance of cortical regions and connections that are vital in linking different functions in the brain network. We observed that cortical regions with multimodal functions tend to have high nodal centrality ( $N_{bc}$ ) and are predominantly intermodular connectors. Those cortical regions are consistent with the hub regions defined in previous human brain functional networks (Achard et al. 2006) and a structural network (He, Chen, et al. 2007). On the other hand, intermodular connections tend to have higher edge centrality ( $E_{bc}$ ) and connect cortical regions with high  $N_{bc}$ . The overlap between these 2 observations is not surprising given the fact that both modular connectors and intermodular connections are more likely to reside on the

shortest paths between any 2 regions that are in different functional modules. However, the  $E_{bc}$  statistic also reveals vital intramodular paths between a high  $N_{bc}$  node and a relatively low  $N_{bc}$  node, for example, MTG.L-SMG.L and PrCG.L-CING.L links, a finding that suggests that  $E_{bc}$  might be able to provide a more detailed evaluation on the importance of a node in the network.

The identification of critical inter- and intramodular cortical regions and connections allows us to identify the structural bottlenecks and preferred pathways that constrain the flow of activity in specific patterns, contributing critically to network functional expression and coordination dynamics (Bressler and Tognoli 2006). The modular architecture of the cortical network might provide a functional explanation as to why changes in the core paths (high  $E_{bc}$ ) and hub regions (high  $N_{bc}$ ) have more profound effects on the stability and efficiency of the brain network than the noncore paths and nonhub regions (Kaiser and Hilgetag 2004; Achard et al. 2006; He, Chen, et al. 2007).

Several methodological considerations need to be addressed. First, we used interregional cortical thickness correlations to represent the human brain structural network. The exact biological nature of the cortical thickness correlations is still unknown, though it has been suggested that regional morphological covariations such as brain tissue volume may be attributed to the mutually trophic influences (Ferrer et al. 1995), the contribution of heredity (Suddath et al. 1990; Steinmetz et al. 1994; Thompson et al. 2001), or environment-related plasticity (Maguire et al. 2000; Draganski et al. 2004; Mechelli et al. 2004). Although not answering the question of what caused these cortical correlation patterns, GRETNA provides a framework for human brain structural organization (He, Chen, et al. 2007) that reflects functional neuroanatomy. Second, numerous module detection algorithms have been developed, and different algorithms could yield different results. However, we compared our results with those obtained with a simulated annealing approach (Guimera and Nunes Amaral 2005) and found minimal difference in modular categorization with the only exception in the module assignment of IFG. Hence, the uncovered network modules appear to be robust. Third, cortical regions in our study are defined by a prior volumetric template that was employed to automatically parcellate the entire cerebral cortex into different regions (Collins et al. 1995). A different cortical parcellation template was applied in recent human brain functional network studies (Salvador et al. 2005; Achard et al. 2006; Achard and Bullmore 2007). The use of different parcellation schemes might cause subtle change of network organization, though the essential modular architecture for any cortical parcellation based on commonly accepted gyral/lobar boundaries should remain intact.

Further investigations will include examining the brain structural network modularity using other cortical morphological features such as local area, volume, or complexity. In future applications, it will be important to investigate how the roles of different modules differ in various settings such as development (Shaw et al. 2006), aging (Sowell et al. 2003), dementia (Desgranges et al. 1998; Buckner et al. 2005; He, Wang, et al. 2007), learning (Draganski et al. 2004), rehabilitation (Han et al. 2007), and psychiatric disorders of connectivity (Honey et al. 1999; Buchanan et al. 2004).

## Conclusion

By exploring a rich and static cortical morphometric database, we found patterns of morphological variation in thickness

across the cortical surface that might be associated with the intrinsic functional modularity of the brain network. This is probably due to the fact that cortical thickness and its inter-regional correlations may reflect the underlying cytoarchitecture and neural connectivity. Analysis of correlation patterns of the cortical structure may thus provide unique and valuable insight into the understanding of the normal cerebral development and cortical abnormalities in various neuropsychiatric disorders. Furthermore, the underlying modular organization, postulated to result from the evolutionary constraints, may reflect the fundamental design principles governing the structure and function of the human brain.

### Supplementary Material

Supplementary material can be found at: <http://www.cercor.oxfordjournals.org/>

### Funding

Human Brain Project (PO1MHO52176-11); Canadian Institutes of Health Research (MOP-34996); Killam Foundation; Montreal Neurological Institute (Jeanne Timmins Costello Fellowship to Y.H.).

### Notes

*Conflict of Interest.* None declared.

Address correspondence to Alan C. Evans, McConnell Brain Imaging Centre, Montreal Neurological Institute, Montreal QC Canada H3A 2B4. Email: [alan.evans@mcgill.ca](mailto:alan.evans@mcgill.ca)

### References

Achard S, Bullmore E. 2007. Efficiency and cost of economical brain functional networks. *PLoS Comput Biol.* 3:e17.

Achard S, Salvador R, Whitcher B, Suckling J, Bullmore E. 2006. A resilient, low-frequency, small-world human brain functional network with highly connected association cortical hubs. *J Neurosci.* 26:63–72.

Amunts K, Schlaug G, Schleicher A, Steinmetz H, Dabringhaus A, Roland PE, Zilles K. 1996. Asymmetry in the human motor cortex and handedness. *Neuroimage.* 4:216–222.

Bassett DS, Meyer-Lindenberg A, Achard S, Duke T, Bullmore E. 2006. Adaptive reconfiguration of fractal small-world human brain functional networks. *Proc Natl Acad Sci USA.* 103:19518–19523.

Bressler SL, Tognoli E. 2006. Operational principles of neurocognitive networks. *Int J Psychophysiol.* 60:139–148.

Buchanan RW, Francis A, Arango C, Miller K, Lefkowitz DM, McMahon RP, Barta PE, Pearlson GD. 2004. Morphometric assessment of the heteromodal association cortex in schizophrenia. *Am J Psychiatry.* 161:322–331.

Buckner RL, Snyder AZ, Shannon BJ, LaRossa G, Sachs R, Fotenos AF, Sheline YI, Klunk WE, Mathis CA, Morris JC, et al. 2005. Molecular, structural, and functional characterization of Alzheimer's disease: evidence for a relationship between default activity, amyloid, and memory. *J Neurosci.* 25:7709–7717.

Burton MW, Locasto PC, Krebs-Noble D, Gullapalli RP. 2005. A systematic investigation of the functional neuroanatomy of auditory and visual phonological processing. *Neuroimage.* 26:647–661.

Cavanna AE, Trimble MR. 2006. The precuneus: a review of its functional anatomy and behavioural correlates. *Brain.* 129: 564–583.

Clauset A, Newman ME, Moore C. 2004. Finding community structure in very large networks. *Phys Rev E Stat Nonlin Soft Matter Phys.* 70:066111.

Collins DL, Holmes CJ, Peter TM, Evans AC. 1995. Automatic 3D model-based neuroanatomical segmentation. *Hum Brain Mapp.* 33: 190–208.

Danon L, Diaz-Guilera A, Arenas A. 2006. The effect of size heterogeneity on community identification in complex networks. *J Stat Mech.* P11010.

Desgranges B, Baron JC, de la Sayette V, Petit-Taboue MC, Benali K, Landeau B, Lechevalier B, Eustache F. 1998. The neural substrates of memory systems impairment in Alzheimer's disease. A PET study of resting brain glucose utilization. *Brain.* 121(Pt 4):611–631.

Downing PE, Wiggett AJ, Peelen MV. 2007. Functional magnetic resonance imaging investigation of overlapping lateral occipitotemporal activations using multi-voxel pattern analysis. *J Neurosci.* 27:226–233.

Draganski B, Gaser C, Busch V, Schuierer G, Bogdahn U, May A. 2004. Neuroplasticity: changes in grey matter induced by training. *Nature.* 427:311–312.

Duncan J, Owen AM. 2000. Common regions of the human frontal lobe recruited by diverse cognitive demands *Trends Neurosci.* 23: 475–483.

Ferrer I, Blanco R, Carulla M, Condom M, Alcantara S, Olive M, Planas A. 1995. Transforming growth factor-alpha immunoreactivity in the developing adult brain. *Neuroscience.* 66:189–199.

Fortunato S, Barthelemy M. 2007. Resolution limit in community detection. *Proc Natl Acad Sci USA.* 104:36–41.

Freeman LC. 1977. Set of measures of centrality based on betweenness. *Sociometry.* 40:35–41.

Genovese CR, Lazar NA, Nichols T. 2002. Thresholding of statistical maps in functional neuroimaging using the false discovery rate. *Neuroimage.* 15:870–878.

Girvan M, Newman ME. 2002. Community structure in social and biological networks. *Proc Natl Acad Sci USA.* 99:7821–7826.

Guimera R, Nunes Amaral LA. 2005. Functional cartography of complex metabolic networks. *Nature.* 433:895–900.

Guimera R, Sales-Pardo M. 2006. Form follows function: the architecture of complex networks. *Mol Syst Biol* 2:42.

Hampson M, Peterson BS, Skudlarski P, Gatenby JC, Gore JC. 2002. Detection of functional connectivity using temporal correlations in MR images. *Hum Brain Mapp.* 15:247–262.

Han BS, Kim SH, Kim OL, Cho SH, Kim YH, Jang SH. 2007. Recovery of corticospinal tract with diffuse axonal injury: a diffusion tensor image study. *NeuroRehabilitation.* 22:151–155.

Hartwell LH, Hopfield JJ, Leibler S, Murray AW. 1999. From molecular to modular cell biology. *Nature.* 402:C47–C52.

He Y, Chen ZJ, Evans AC. 2007. Small-world anatomical networks in the human brain revealed by cortical thickness from MRI. *Cereb Cortex.* 17:2407–2419.

He Y, Wang L, Zang Y, Tian L, Zhang X, Li K, Jiang T. 2007. Regional coherence changes in the early stages of Alzheimer's disease: a combined structural and resting-state functional MRI study. *Neuroimage.* 35:488–500.

Hilgetag CC, Burns GA, O'Neill MA, Scannell JW, Young MP. 2000. Anatomical connectivity defines the organization of clusters of cortical areas in the macaque monkey and the cat. *Philos Trans R Soc Lond B Biol Sci.* 355:91–110.

Honey GD, Bullmore ET, Soni W, Varatheesan M, Williams SC, Sharma T. 1999. Differences in frontal cortical activation by a working memory task after substitution of risperidone for typical antipsychotic drugs in patients with schizophrenia. *Proc Natl Acad Sci USA.* 96: 13432–13437.

Iserberg N, Silbersweig D, Engelien A, Emmerich S, Malavade K, Beattie B, Leon AC, Stern E. 1999. Linguistic threat activates the human amygdala. *Proc Natl Acad Sci USA.* 96:10456–10459.

Kaiser M, Hilgetag CC. 2004. Edge vulnerability in neural and metabolic networks. *Biol Cybern.* 90:311–317.

Kier EL, Staib LH, Davis LM, Bronen RA. 2004. MR imaging of the temporal stem: anatomic dissection tractography of the uncinate fasciculus, inferior occipitofrontal tractoculus, and Meyer's loop of the optic radiation. *AJNR Am J Neuroradiol.* 25:677–691.

Kotter R, Stephan KE. 2003. Network participation indices: characterizing component roles for information processing in neural networks. *Neural Netw.* 16:1261–1275.

Latora V, Marchiori M. 2001. Efficient behavior of small-world networks. *Phys Rev Lett.* 87:198701.

- Lerch JP, Worsley K, Shaw WP, Greenstein DK, Lenroot RK, Giedd J, Evans AC. 2006. Mapping anatomical correlations across cerebral cortex (MACACC) using cortical thickness from MRI. *Neuroimage*. 31:993-1003.
- Lieberman P. 1998. *Eve spoke: human language and human evolution*. New York: WW Norton.
- Lowe MJ, Mock BJ, Sorenson JA. 1998. Functional connectivity in single and multislice echoplanar imaging using resting-state fluctuations. *Neuroimage*. 7:119-132.
- Luppino G, Rizzolatti G. 2000. The organization of the frontal motor cortex. *News Physiol Sci*. 15:219-224.
- Maguire EA, Gadian DG, Johnsrude IS, Good CD, Ashburner J, Frackowiak RS, Frith CD. 2000. Navigation-related structural change in the hippocampi of taxi drivers. *Proc Natl Acad Sci USA*. 97:4398-4403.
- Maslov S, Sneppen K. 2002. Specificity and stability in topology of protein networks. *Science*. 296:910-913.
- Mazziotta J, et al. 2001. A probabilistic atlas and reference system for the human brain: International Consortium for Brain Mapping (ICBM). *Philos Trans R Soc Lond B Biol Sci*. 356:1293-1322.
- Mechelli A, Friston KJ, Frackowiak RS, Price CJ. 2005. Structural covariance in the human cortex. *J Neurosci*. 25:8303-8310.
- Mechelli A, Crinion JT, Noppeney U, O'Doherty J, Ashburner J, Frackowiak RS, Price CJ. 2004. Neurolinguistics: structural plasticity in the bilingual brain. *Nature*. 431:757.
- Mesulam MM. 1985. *Principles of behavioral neurology*. Philadelphia (PA): F A Davis Company: 1-70.
- Mesulam MM. 1990. Large-scale neurocognitive networks and distributed processing for attention, language, and memory. *Ann Neurol*. 28:597-613.
- Mesulam MM. 2000. *Principles of behavioral and cognitive neurology*. New York: Oxford University Press: 1-91.
- Micheloyannis S, Pachou E, Stam CJ, Vourkas M, Erimaki S, Tsirka V. 2006. Using graph theoretical analysis of multi channel EEG to evaluate the neural efficiency hypothesis. *Neurosci Lett*. 402:273-277.
- Newman ME. 2006. Modularity and community structure in networks. *Proc Natl Acad Sci USA*. 103:8577-8582.
- Newman MEJ. 2004. Fast algorithm for detecting community structure in network. *Phys Rev E*, 69, 066133.
- Parent A, Carpenter M. 1995. *Human neuroanatomy*. Baltimore (MD): Williams & Wilkins.
- Salvador R, Suckling J, Coleman MR, Pickard JD, Menon D, Bullmore E. 2005. Neurophysiological architecture of functional magnetic resonance images of human brain. *Cereb Cortex*. 15:1332-1342.
- Scannell JW, Blakemore C, Young MP. 1995. Analysis of connectivity in the cat cerebral cortex. *J Neurosci*. 15:1463-1483.
- Scannell JW, Burns GA, Hilgetag CC, O'Neil MA, Young MP. 1999. The connective organization of the cortico-thalamic system of the cat. *Cereb Cortex*. 9:277-299.
- Serrien DJ, Ivry RB, Swinnen SP. 2006. Dynamics of hemispheric specialization and integration in the context of motor control. *Nat Rev Neurosci*. 7:160-166.
- Shaw P, Greenstein D, Lerch J, Clasen L, Lenroot R, Gogtay N, Evans A, Rapoport J, Giedd J. 2006. Intellectual ability and cortical development in children and adolescents. *Nature*. 440:676-679.
- Sowell ER, Peterson BS, Thompson PM, Welcom SE, Henkenius AL, Toga AW. 2003. Mapping cortical change across the human life span. *Nat Neurosci*. 6:309-315.
- Sporns O, Tononi G, Edelman GM. 2000. Theoretical neuroanatomy: relating anatomical and functional connectivity in graphs and cortical connection matrices. *Cereb Cortex*. 10:127-141.
- Sporns O, Tononi G, Kotter R. 2005. The human connectome: a structural description of the human brain. *PLoS Comput Biol*. 1:e42.
- Sporns O, Chialvo DR, Kaiser M, Hilgetag CC. 2004. Organization, development and function of complex brain networks. *Trends Cogn Sci*. 8:418-425.
- Stam CJ. 2004. Functional connectivity patterns of human magnetoencephalographic recordings: a 'small-world' network? *Neurosci Lett*. 355:25-28.
- Stam CJ, Jones BF, Nolte G, Breakspear M, Scheltens P. 2007. Small-world networks and functional connectivity in Alzheimer's disease. *Cereb Cortex*. 17:92-99.
- Steinmetz H, Herzog A, Huang Y, Hacklander T. 1994. Discordant brain-surface anatomy in monozygotic twins. *N Engl J Med*. 331:951-952.
- Suddath RL, Christison GW, Torrey EF, Casanova MF, Weinberger DR. 1990. Anatomical abnormalities in the brains of monozygotic twins discordant for schizophrenia. *N Engl J Med*. 322:789-794.
- Thompson PM, Cannon TD, Narr KL, van Erp T, Poutanen VP, Huttunen M, Lonnqvist J, Standertskjold-Nordenstam CG, Kaprio J, Khaledy M, et al. 2001. Genetic influences on brain structure. *Nat Neurosci*. 4:1253-1258.
- Wang L, Zang Y, He Y, Liang M, Zhang X, Tian L, Wu T, Jiang T, Li K. 2006. Changes in hippocampal connectivity in the early stages of Alzheimer's disease: evidence from resting state fMRI. *Neuroimage*. 31:496-504.
- Watkins KE, Paus T, Lerch JP, Zijdenbos A, Collins DL, Neelin P, Taylor J, Worsley KJ, Evans AC. 2001. Structural asymmetries in the human brain: a voxel-based statistical analysis of 142 MRI scans. *Cereb Cortex*. 11:868-877.
- Zhou C, Zemanova L, Zamora G, Hilgetag CC, Kurths J. 2006. Hierarchical organization unveiled by functional connectivity in complex brain networks. *Phys Rev Lett*. 97:238103.